Alpha-Particle-Induced Soft Errors in Dynamic Memories

TIMOTHY C. MAY, MEMBER, IEEE, AND MURRAY H. WOODS

Abstract—A new physical soft error mechanism in dynamic RAM's and CCD's is the upset of stored data by the passage of alpha particles through the memory array area. The alpha particles are emitted by the radioactive decay of uranium and thorium which are present in parts-per-million levels in packaging materials. When an alpha particle penetrates the die surface, it can create enough electron-hole pairs near a storage node to cause a random, single-bit error. Results of experiments and measurements of alpha activity of materials are reported and a physical model for the soft error is developed. Implications for the future of dynamic memories are also discussed.

I. INTRODUCTION

THE SEMICONDUCTOR industry has seen a continuing trend toward higher levels of integration in memory circuits. Random-access memories (RAM's) have progressed from the 1K dynamic RAM with a 3-transistor cell, introduced in 1971, to the single-transistor cell 4K dynamic RAM, introduced in 1974, to the "half-transistor" cell 16K dynamic RAM first introduced in 1976. Even denser 64K-bit RAM's are now being designed and we can expect the density trend to continue with no end immediately in sight.

Charge-coupled devices (CCD's) have shown a similar trend, with 16K devices introduced in 1974 and 64K devices now being sampled.

These increased levels of integration have generally been achieved through a reduction of storage cell size with corresponding improvement in sense amplifier sensitivity.

We will show in this paper that a fundamental, error-producing physical mechanism may provide the ultimate limit to this trend toward smaller stored charge packets. This mechanism is the upset of stored data in dynamic memories by ionizing radiation, producing a soft error.

We define "soft errors" to be random, nonrecurring, single-bit errors in memory devices. The errors are not permanent, i.e., no physical defects are associated with the failed bit. In fact, a bit showing a soft error is completely recovered by the following write cycle with no greater chance of showing an error than any other bit in the device.

Soft errors in dynamic memory systems have previously been identified as being caused by either "system noise," "voltage marginality," "sense amplifiers," or "pattern sensitivity." However, the phenomenon we are reporting is a physical, rather than a statistical, mechanism. When soft error rates are discussed in the context of this work, it is with the assumption that the sources mentioned above have been eliminated. The significance of this mechanism is that it cannot be eliminated by standard noise-reduction procedures; only proper design of the memory device itself can eliminate these soft errors.

Dynamic memories store data as the presence or absence of minority carrier charge on storage capacitors. Refresh is required to maintain the stored charge. For n-channel MOS RAM's and CCD's the charges are electrons, and capacitors take the form of potential wells in the p-type silicon under positively charged polysilicon gate electrodes. The amount of charge which can be stored is typically in the range of 300 000 to 3 000 000 electrons. However, the number of electrons which differentiates between "empty" and "full" wells is reduced from the above amounts by such effects as: incomplete charge transfer to sense amp bit lines, sense amp sensitivity, and thermal generation. The number of electrons which differentiates between a "1" and "0" we define as the "critical charge," Q_{crit}.

The refresh failure of empty wells in dynamic memories to hold their data either when exposed to enough light or to a high enough temperature is due to their filling up with generated electrons. As we will show, the physical mechanism for the soft errors is similar to this type of "refresh failure," except that the electrons are being generated by ionizing radiation.

Electron-hole pairs are generated by the alpha particles as they lose energy in the silicon and can be collected by depletion layers such that the generated electrons end up in storage wells. If the fraction collected times the number generated exceeds Q_{crit}, a "soft error" will result. One alpha particle is capable of causing a soft error in some sensitive 4K and 16K RAM's. Results of a number of experiments on devices with reduced geometries and operating voltages indicate that 64K-bit RAM's and CCD's will show appreciable soft error rates unless corrective actions are taken to reduce their sensitivity to alpha-induced upset.

Section II will present the basic physical model. Section III discusses experimental evidence in support of the model. Section IV reports on the sources of alpha particles in packaging materials. Factors affecting soft error rates will be examined in more detail in Section V and the results will be used to predict the soft error rate of a particular 4K test structure in Section VI. Finally, some conclusions will be drawn and implications for 64K-bit devices and beyond will be discussed.

Manuscript received June 27, 1978; revised September 27, 1978.
The authors are with Intel Corporation, Santa Clara, CA 95051.

0018-9383/79/0100-0002$00.75

II. Physical Model

A number of system experiments with dynamic memories containing up to 64K-bits have been done to confirm that soft errors can be caused by alpha particles. In addition, artificial sources such as polonium-210 and thorium-230 as well as natural sources such as uranium/thorium minerals have been used to produce soft errors in sensitive test structures. These experiments are fully consistent with expectation from the basic model presented in this section and will be reported in the next section, on "Experimental Evidence." An introduction to the physical mechanism will clarify the experiments.

Alpha Particles

Alpha particles are doubly charged helium nuclei (2 protons, 2 neutrons) ejected from the nucleus of high-Z atoms during radioactive decay. They range in energy up to about 8-9 MeV for all naturally occurring elements that undergo alpha decay. Fig. 1 plots the range of alpha particles in silicon as a function of incident energy. The ranges in SiO_2, Al, etc., are well known and are within a factor of two of the range in silicon [1].

Alphas interact heavily with matter because of their charge. A 4-MeV alpha entering Si initially has a speed of 0.05 c and loses energy at a rate of dE/dx = 150 keV/μm [1]. The total ionization produced is determined by the initial particle energy and the average energy per ion pair. This number has been measured for generation by highly energetic particles to be 3.6 eV/electron-hole pair [1].

Other alphas properties critical to soft error modeling:

Alphas travel in nearly straight lines.

The "straggling," or scatter in range is small (for a range R essentially all alphas stop between 0.98R and 1.02R).

Alphas are emitted at discrete energies. However, as will be shown in Fig. 6, self-absorbtion by sources thicker than the range will produce a continuum of measured alpha energies from the maximum energy of emission down to zero.

Alpha emissions are nuclear events and are unaffected by temperature, pressure, etc.

The electron-hole pair generation takes place within 2-3 μm of the alpha track [2].

It is fortuitous that alpha particles have ranges comparable with current device dimensions and can create numbers of electron-hole pairs comparable to the number required to upset data in some dynamic memories. This is of course the reason this mechanism has only recently become evident—previous generations of devices were too big to be affected by naturally occuring alphas.

Beta and gamma sources are not expected to produce soft errors because of their relatively low energy loss rates in silicon. Indeed, this was confirmed by experiments with intense beta and gamma sources which produced no soft errors in hours of exposure (though extremely intense sources did produce catastrophic threshold shifts after long periods).

The possibility that sea-level cosmic rays can cause upset is less easily dismissed [3], [4]. Solid-state particle detectors consisting of n^+-p structures with extremely deep collecting regions are constantly detecting cosmic rays as "background."

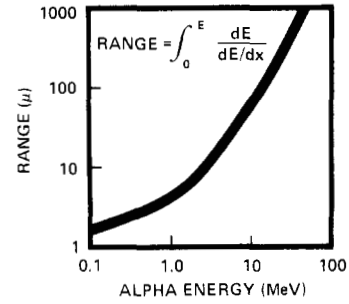

Fig. 1. Range of alpha particles in Si.

Experimental evidence indicates that most (>90 percent) soft errors seen in devices from several manufacturers are due to alpha particles from package materials. System experiments with a 20 ton "lead cave" are being undertaken in order to determine if cosmic rays can contribute significantly to soft error rates. Preliminary results indicate that 64K CCD's are affected by the flux of high-Z cosmic rays at sea level; these experiments will be reported in a future paper.

Electron-Hole Pair Collection

Up to 2.5×10^6 electron-hole pairs can be generated in a period of several picoseconds by the passage of the highest energy, naturally occurring alpha particle. Those generated in the surface layers of a device (SiO_2, phosphosilicate glass, etc.) are not collected. The 2-4-μm thickness results in an average loss of about 200 keV of alpha energy and thus has no significant effect on the energy deposited in the silicon, except at low angles of incidence.

Carriers generated in depletion layers surrounding diffusions or under gate regions are separated by electric fields. For n-channel technologies, electrons are swept into storage wells and holes into the substrate. The "collection efficiency," defined to be the ratio of carriers collected to the total number generated in a region, is near unity in this region, limited only by the relatively small amount of recombination which goes on.

Electrons and holes generated outside of depletion regions diffuse through the bulk silicon. For those which reach the edge of the depletion layer, the electrons are swept into the storage regions and the holes are ohmically relaxed through the substrate contact. An exact solution of the diffusion equation shows the collection currents peak very rapidly after generation in the bulk and the collection process is complete within microseconds.

All of the features of the simple model are brought together in Fig. 2. The "potential wells" shown in the figures should not be confused with actual depletion region geometries—the "empty" and "full" wells are shown for pedagogical reasons. The effective electron collection volume depends on the depletion region dimensions and on the minority carrier diffusion length and is not related to the "potential wells" discussed here. It is clear that the actual soft error rate of a particular test structure or actual device depends on a number of factors: flux and energy of ionizing radiation, target area, critical charge, collection efficiency,

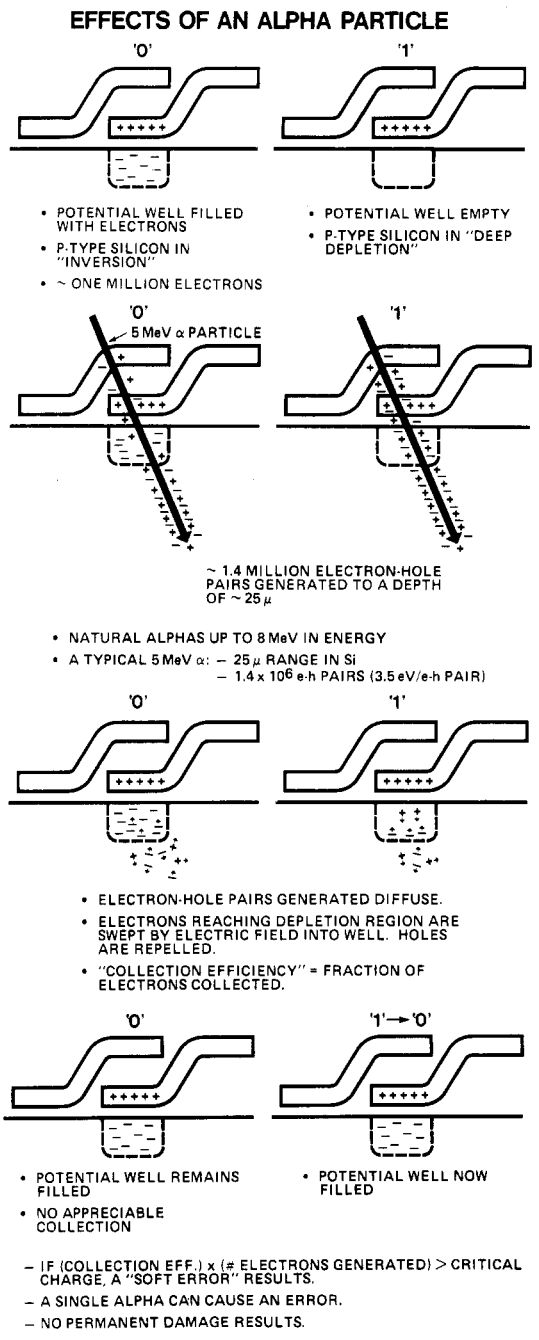

Fig. 2. Stages of soft error creation by alpha particles in dynamic memories.

cell geometry, etc. These, in turn, are a function of device design and technology parameters and the package type and composition.

III. Experimental Evidence

In order to fully understand and characterize the soft error rate of various devices a total of greater than 25 million device hours incorporating various data patterns were accumulated in a read-only mode, error-logging system test. Additionally, single device studies were performed by exposing the die to intense alpha sources and monitoring the error rates on raster scanning systems. Finally, to understand the effects of device design, geometry, and other properties on soft error rates, memory arrays and test structures ranging from 1K to 64K-bits were tested. Included in these studies were special geometric shrinks and arrays with sense amp changes, gate oxide changes, or operating voltage changes.

The system error rate data form the basis for one very compelling piece of evidence for the correctness of our soft error model. That is, theoretical calculations for soft error rates of specific arrays in specific package environments agree very closely with measured system soft error rates. The model also predicts four other major results that can be tested in order to verify the model:

1) Errors should be randomized to single bits and non-recurring.

2) Errors should occur only when empty potential wells collect electrons.

3) Error rate should be proportional to the alpha flux.

4) Error rate should be strongly dependent on critical charge.

The first two results have been confirmed for certain dynamic arrays by raster scans of single devices incorporating a half "1's", half "0's" data pattern. When these arrays were exposed to intense 5 mCi (1 Ci = 3.7×10^{10} disintegrations/s) Po-210 alpha sources with maximum alpha energy of 5.31 MeV, only half of the array with a solid "1's" (empty well) data pattern exhibited soft errors, which were randomly distributed. Not all dynamic memories show only $1 \rightarrow 0$ soft errors. For example, if the data pattern is inverted internally, it can appear externally as if a $0 \rightarrow 1$ soft error has occurred. Also, in some devices, electrons collected by floating nodes in other portions of the circuitry can contribute to soft errors. For example, the bit sense line in 16K RAM's is precharged to some voltage and then left floating for a period of tens of nanoseconds prior to readout of cell information. During this period, the bit sense line is capable of collecting electrons which may result in either a soft error on "1's" in the cell or "0's" in the cell. Although the time for charge collection is short, the collection area is sufficiently large to result in the bit-line mode dominating the cell mode for most current-generation 16K RAM's.

Some static RAM's, particularly low-power devices with polysilicon load resistors, are also showing soft errors. Again, the mechanism is the collection of charge by floating nodes.

Alpha-Flux Experiments

Again, both systems and artificial source experiments were performed. The error rate was confirmed to be directly proportional to the alpha flux over 8 decades of source intensity. Fig. 3 shows results for a 4K test device for various flux levels. The 4K test device has a small Q_{crit} (less than 750 000 electrons). A second 4K array with a Q_{crit} approximately 2 times larger is also shown.

The commercially available intense sources used were 10 mCi, 5 mCi, 3 mCi, and 0.1 μCi Po-210 sources. Acquisition of statistically valid data took little time with the two most intense sources but took several hours per test device with the 0.1-μCi source.

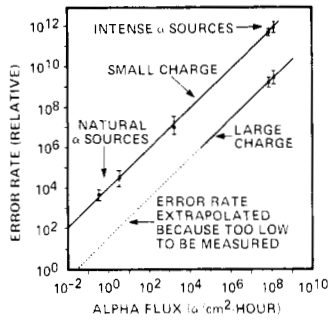

Fig. 3. Error rate versus alpha flux for two test devices of different critical charges.

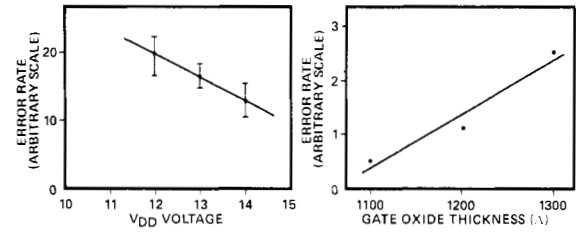

Fig. 4. Effects of critical charge on soft error rate. (a) Critical charge proportional to operating voltages. (b) Critical charge proportional to oxide capacitance.

The linearity of the error rate for these test devices, and for others, over 8 decades of source intensity, is compelling evidence that the alpha flux in packaged devices is sufficient to account for observed soft error rates in memory systems.

Another experiment to track soft errors with alpha activity used ceramic package lids fully glazed with a known "hot" glass. These were taped in place over a test device in place of the normal lids and the soft error rate increased from the typical 1-3 percent/1000-h level for this test device to over 1300 percent/1000 h. This is fully consistent with the flux increase from 0.03-0.07 $\alpha/cm^2 \cdot h$ to over 35 $\alpha/cm^2 \cdot h$. Controls with "cold" lids taped in place showed no increase in error rate, showing that neither loss of hermeticity, nor stray light leakage, nor any other effects related to merely removing the original lids had any significant effect on the experiment.

Furthermore, placing masking tape on the underside of the "hot" lids reduced the soft error rate to the prior low levels. This was important as further confirmation of the alpha-particle hypothesis, inasmuch as a 5-mil thickness of masking tape will stop all alphas but will have negligible effect on beta particles and gamma rays emitted by the radioactive glass.

A note on this procedure: The technique of using intense alpha sources has the advantage of allowing much faster data taking on the sensitivity of a particular device or on the effects of design/technology changes, operating voltages, angle of incidence, etc., but it has several drawbacks which limit its usefulness:

1) The energy spectrum of polonium and americium intense alpha sources differs from the spectrum from natural U/Th sources. The differences are in maximum alpha energies and in the shapes of the spectra. For devices with very low Q_{crit} the results are correlatable, but for devices designed to have a larger Q_{crit} the results of a polonium or americium "lab test" can be misleading because devices with large Q_{crit} may fail when exposed to U/Th alphas but not fail with Po-210 or Am-241 alphas.

2) As flux increases, the probability of a bit being hit two or more times within the same refresh period ceases to be negligible. Calculation of this probability is a straightforward application of Poisson statistics. Multiple hits are negligible for the low flux levels seen in packaged devices.

3) Threshold shifts and increased surface state density can occur under prolonged exposure to intense sources. When this happens, after a period of exposure time the soft error rate will begin to increase (e.g., tens of minutes exposure to a millicurie source of Po-210).

4) A note of *warning:* Experiments with Po-210 intense sources should not be done above room temperature because polonium begins to volatilize at 50-60°C and is extremely *toxic*.

Critical Charge Experiments

The charge stored in a dynamic memory can be varied by changing cell geometry and hence storage capacitance, or by changing voltages.

Fig. 4(a) shows the dependence of soft error rate on the V_{DD} voltage applied to a 16K charge-coupled device (CCD). As expected, because of increased critical charge, the soft error rate declined with increased gate voltage. However, increased voltages also produce unacceptably high hard error rates due to oxide breakdown.

In another critical charge experiment, 16K CCD's were fabricated with 3 different gate oxide thicknesses: 1100, 1200, and 1300 Å. The soft error rate increased with increasing gate oxide thickness, as would be expected from the decreasing charge storage capability. Fig. 4(b) shows results of this experiment.

In yet another experiment, a current-generation 4K RAM was fabricated with a 20-percent linear shrink in storage capacitor dimensions, resulting in a 500X increase in the soft errors.

From the results of these experiments and from the theory itself, the role of critical charge in determining soft error rates is clear: Critical charge is the most important factor in determining device sensitivity to soft errors.

In fact, plotting measured soft error rates versus estimated Q_{crit} for a number of dynamic RAM's and CCD's from several manufacturers results in the trend shown in Fig. 5. Again it can be seen that devices with smaller critical charges exhibit higher soft error rates. The critical charges, in millions of electrons, are accurate to about ±20 percent and are based on measured cell geometries and estimated sense margins. The error rates were measured either in systems with error detection or in laboratory measurements with alpha sources of known intensity. These latter measurements were corrected for the ratio of source intensity to package source intensity. The measured soft error rates are accurate to about ±10 percent for each individual device, but scatter within a group of devices limits accuracy to about an order of magnitude.

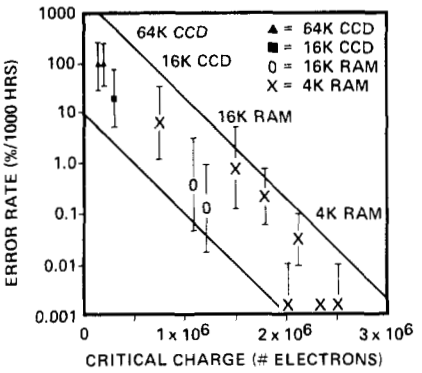

Fig. 5. Error rate versus critical charge for devices from several manufacturers.

The error rate versus Q_{crit} is not expected to be completely linear since no corrections have been made for cell geometry, package type, collection efficiency, etc. That the correlation between soft error rate and Q_{crit} is as strong as it is, is evidence that critical charge is the dominant factor. Other factors are second-order in determining the error rate in a known alpha flux.

The roughly logarithmic falloff in error rate with increasing Q_{crit} is expected because of the rapidly decreasing number of alphas capable of causing cell upset as Q_{crit} increases.

IV. Materials Analysis

Following confirmation of the alpha-particle hypothesis, an extensive program to identify the alpha sources was begun.

Measurement Techniques

Radioactivity levels of package materials, measured in "picocuries per gram" (1 Ci = 3.7×10^{10} disintegrations/s), were obtained with gamma counters and verified by gas-proportional counters. Alpha-particle fluxes (in $\alpha/cm^2 \cdot h$) were measured with scintillation alpha counters. Extremely low level alpha fluxes were measured with nuclear emulsion and cellulose nitrate track counting techniques [5]. The alpha-particle energy spectrum for different materials was obtained with a silicon surface-barrier detector and a microprocessor-based multichannel analyzer (MCA). Fig. 7, to be further discussed in Section V, shows a typical energy spectrum from zirconia, a primary source of radioactivity in packages. This procedure was important both in confirming alpha activity to be due to U/Th and in providing the true number of alphas available at various energies (needed for the physical model).

Quantitative analysis methods ranging from simple energy-dispersive X-ray analysis, to emission spectrographic analysis, to mass spectrometry were used to obtain concentrations of elements in various materials. Precise isotopic abundances were determined for some samples, to be certain that the primary radioactive species were in fact U-238, U-235, and Th-232.

A note on the measurement errors: For very-low flux levels, counting times of weeks were necessary to separate out the background count and to obtain a statistically significant 95-percent confidence level.

TABLE I
Materials Analysis

Material	ppmU(1)	ppmTh(2)	α/cm²-hour(3)	% Zr(4)
Alumina - A	2.5	0.6	0.6	1
Alumina - B	-	-	0.3	-
Alumina - C	-	-	0.5	-
Glass - A	12	6	29	17.5
Glass - B	2.5	3	5.2	3
Glass - C	17	6	45	25
Glass - D	12	6	18	6
Glass - E	-	-	32	20
Epoxy	-	-	1.7	-
Silicone	-	-	1.3	-
Au-Plated Lids	-	-	.04-1.0(5)	-

(1),(2) Mass spectrographic analysis.
(3) Alpha scintillation counting.
(4) Emission spectrographic analysis.
(5) Activity varied widely.

Results of Analysis

Table I lists the major results. Listed with each material are the concentrations of uranium and thorium in parts per million (weight), the percentage of zirconium, and the measured alpha flux.

The sealing glasses, typically oxides of Pb, Al, Zn, etc., show the widest spread in activity and the highest peak levels, ranging from about 1 $\alpha/cm^2 \cdot h$ to over 45 $\alpha/cm^2 \cdot h$ for a glass now in widespread use by the semiconductor industry. The zirconia filler material was found to be the chief source of U and Th, consistent with published results [6]. Alumina (Al_2O_3) from side-brazed ceramic and cerdip packages is also found to contain trace amounts of U and Th. Even the gold-plated metal lids used in side-brazed packages were found to show alpha activity.

Plastic packages contain fillers, usually quartz, and which contain uranium and thorium up to 1-2 ppm. Soft error rates for several devices in plastic packages were consistent with the measured alpha flux.

The correlation between U/Th concentration and measured alpha flux indicated in Table I can be predicted by a simple calculation which takes into account the following: 1) range of alphas in source material, 2) 25 percent within one range escape, 3) density of source material, 4) half-life of U/Th, and 5) number of alphas in decay sequence. The percent Zr is also of use, since approximately 1 in 10^4 Zr atoms are replaced by uranium or thorium atoms [7]; it is, therefore, close to the U/Th parts-per-million level.

Finally, our studies with the MCA show the full spectrum of energy is available in all packaging materials examined. This indicates that chemical processing has not affected the energy spectrum for materials containing approximately the same proportions of U and Th.

V. Error Rate Factors

We know at one extreme that if a device has a sufficiently large Q_{crit} (2.5×10^6 electrons or more) no soft errors will occur with single alpha-particle hits, since no naturally occurring alpha has sufficient energy to create enough electron-

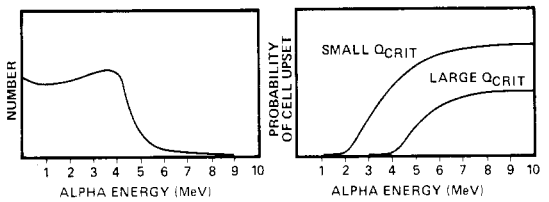

Fig. 6. (a) Alpha-particle spectrum versus energy for material with 50/50 U/Th mix. (b) Dependence of cell upset probability versus alpha energy for devices of different critical charge.

hole pairs. And at the other extreme, we can imagine a device with so small a Q_{crit} (e.g., 50 000 electrons) that essentially all alphas reaching the active area of the device produce one or more soft errors. It is in the range in between these extremes where an understanding of other factors, such as alpha flux and energy spectrum, critical charge, collection efficiency, cell geometry, etc., is needed. For example, variations in collection efficiency may alter the error rate by orders of magnitude if the device is "borderline" to begin with. The major importance of critical charge was previously discussed. Several of the other important factors are discussed below.

Alpha Flux

Alpha flux at the die surface is easily computed if source intensities and locations relative to the die are known. Solder glass sources are generally in a ring (rectangular) at some height above the die and give rise to a flux through the die which ranges from 0.1 $\alpha/cm^2 \cdot h$ to about 5 $\alpha/cm^2 \cdot h$, depending on glass type. Gold-plated metal lids and ceramic lids act as parallel-plate sources to the die. From Table I, it can be seen that contributions to the total die surface flux from these sources range from less than 0.04 $\alpha/cm^2 \cdot h$ to greater than 1 $\alpha/cm^2 \cdot h$. It is interesting to note that even a relatively low alpha flux such as 0.01 $\alpha/cm^2 \cdot h$ could be enough to produce a >100 percent/1000 h failure rate for a future dynamic memory with a reasonably small Q_{crit} (e.g., 50 000 electrons).

Alpha Energy

Since the alpha-particle energy determines the number of electron-hole pairs generated in the silicon, the alpha energy spectrum is of importance in determining the fraction of alphas capable of causing error.

The decay of U-238 produced 8 alphas in the decay sequence from U-238 to stable Pb-206 [8]. Th-230 produces 6 alphas in its decay to Pb-208. The alphas are emitted at energies ranging from 3.95 to over 9 MeV. A continuous spectrum down to 0 MeV is expected due to emission throughout the region within 40 μm of the surface. Fig. 6(a) shows schematically what is expected for a 50/50 mixture of U and Th. The $N(E)$ curve peaks at 4-5 MeV—beyond that energy the number of alphas drops off sharply. The measured energy spectrum from a zirconia sample is shown in the top trace of Fig. 7. Also, shown in the lower trace of the figure, is the derivative dN/dE which shows the specific alpha energies emitted by uranium and thorium. An important result is that the actual

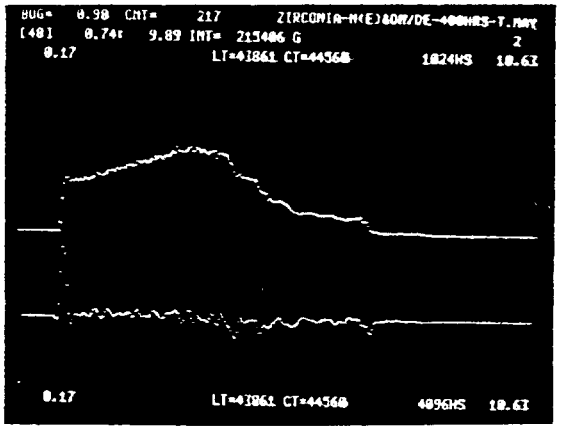

Fig. 7. Alpha energy spectrum from zirconia. Energy scale ranges from 0.17 to 10.63 MeV. Bottom trace is the derivative, dN/dE, which shows specific U/Th alphas.

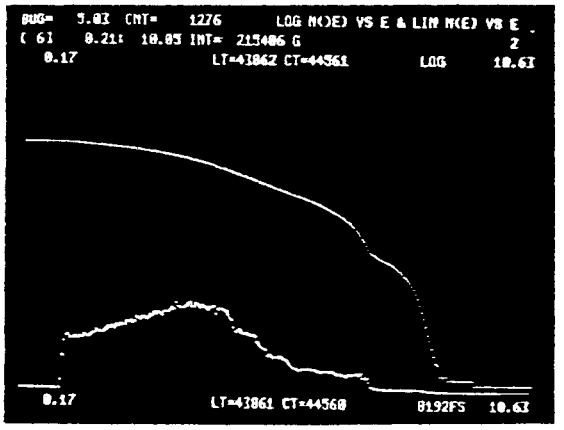

Fig. 8. $N(>E)$ versus E, showing on a *log scale* the number of alphas exceeding a given energy E. Shown for reference is the $N(E)$ spectrum, on a linear scale. $N(>E)$ drops rapidly above 6 MeV.

energy spectra from a number of uranium/thorium minerals and package materials were found to be essentially identical.

The relative importance of different critical charges for various devices can be most readily assessed by considering the fraction of the total alphas exceeding a given energy E. The top trace of Fig. 8 plots the number of alphas exceeding energy E versus E. From this we can understand qualitatively the rapid dropoff in soft error rate as Q_{crit} is increased—the number of alphas capable of causing error drops rapidly with increasing energy.

Collection Efficiency

The collection efficiency is the fraction of the total number of alpha-generated electrons which are collected by storage nodes. It is a function of cell area, point and depth of generation, minority carrier lifetime in the p-region, depletion region dimensions, and trap density. Also, the location and number of other collection regions, which can "compete" for the generated electrons, play a role.

The collection efficiency plays a critical role in the soft error rate because it determines whether a critical charge can be collected from the total number generated. A description

of all collection efficiency experiments involving the above factors is beyond the scope of this paper. However, as an example, the results of a simple experiment are illustrated here. 16K CCD's with and without an anneal (to control minority carrier lifetimes) were tested in a memory system with the result that short-lifetime devices had a lower error rate, due to the reduced collection efficiency.

Cell Geometry

The area of a memory cell is important in the calculation of the total "target area" and is also a factor in the collection efficiency. Large cells will, for the same collection efficiency and Q_{crit}, give a higher soft error rate than small cells. But the size of a cell is generally tied directly to the critical charge size, hence the progression toward denser memories and smaller cell sizes has, with a few recent exceptions, led to decreased Q_{crit}.

If the number of cells per unit area is increased without a proportionate increase in errors/alpha (e.g., the errors/alpha has saturated at unity) then for a given alpha flux the bit error rate actually decreases. However, commercially available 64K CCD's have shown multiple soft errors per alpha (due to the small Q_{crit} and high collection efficiency of buried-channel CCD designs) so that the assumption of "saturation" is not necessarily realistic for all future generations of devices. Experiments indicate that there is a certain level of critical charge (about 750 000 electrons) above which the assumption does hold.

Other Factors

The geometry, composition, and thickness of attenuating oxide passivation layers can affect soft error rates, especially for shallow angles of alpha-particle incidence. The angle at which alpha particles hit the device surface affects not only their attenuation but also their depth of penetration, the collection efficiency for generated carriers, and the effective area the die presents to a flux of incoming alphas. Inasmuch as some of the highest activity sources are located such as to give angles of incidence of 15-30° above the die surface, the study of this angle effect is of more than just scientific interest.

In order to evaluate the effects of alpha-particle incidence angle, a jig was constructed which allows a Po-210 alpha source to be swung in an arc around a test device. The source is collimated with a 3-mm aperture and is about 5 cm from the die. A bell jar surrounds the jig and is evacuated to eliminate air absorbtion of the alphas. All error rates are measured in darkness to eliminate electron-hole pair generation by room light. Several types of devices have been fully characterized at angles from 90° (vertical incidence) to 20° (where the package body begins to obstruct the beam of alphas). The results were as expected: the error rate at 90° was lower than at about 50-60°, where columnar recombination effects are reduced. At lower angles, the error rate was reduced by the sin θ area effect and increased absorbtion in surface layers (a 1/ sin θ effect). Fig. 9 shows results of this angle experiment for one type of device.

Another soft error rate factor relates to refresh periods. Longer times between refresh of a cell can result in a decrease

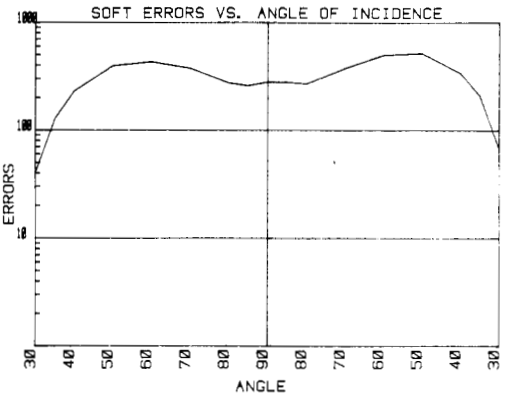

Fig. 9. Soft error rate for 4K test array versus angle of alpha particle incidence.

in Q_{crit} due to thermal generation of electron-hole pairs gradually filling up the potential wells. Other effects related to the refresh time are being investigated and will be reported in the future.

VI. Error Rate Calculations

It is clear that soft error rates in dynamic memories are reduced by separately attacking the various factors which we have shown phenomenologically to affect the device soft error sensitivity. However, the relative importance of each of these factors for a given device can also be demonstrated by theoretical error rate calculations. An error rate calculation can also lend credence to the basic correctness of the soft errors model. A simple calculation to illustrate the basic procedure is included below.

A 4K test device with the memory cells divided equally between "1's" and "0's" has an active area A of 0.027 cm^2.

The alpha flux Φ_α in a glass-sealed ceramic package used for this device, is computed to be 3.8 α/cm^2 · h. The lid contribution is 0.2 α/cm^2 · h and the seal ring contribution is 3.6 α/cm^2 · h. Thus the majority of the alphas strike the die surface at a low angle (15°).

To calculate the "sensitivity factor," the number of errors per alpha, detailed consideration is made of the actual device cross section, the depletion region depth, the collection areas of the n^+ diffusions used to store charge, and the exact energy spectrum of the incoming alphas. The "sensitivity factor," S, is defined to be the fraction of all alphas hitting the active array (at a 15° angle) that causes errors. Therefore

$$S = \begin{pmatrix}\text{Linear fraction that hits on the diffusion portion}\\ \text{of the cell area) X (Probability of } \alpha \text{ of energy } E_i\\ \text{resulting in upset) X (Probability of impinging } \alpha\\ \text{having energy } E_i).\end{pmatrix}$$

Or by breaking the problem into discrete energies we can write

$$S = \frac{A_{storage}}{A_{cell}} \sum_i P(E_i)N(E_i).$$

The probability of cell upset increases with increasing energy (see Fig. 6(b)), but the chance of encountering an alpha of energy E_i decreases with E. The summation converges.

A graphical Monte Carlo technique was used to estimate S

for the known energy spectrum $N(E_i)$ and the known Q_{crit} (which determined $P(E_i)$), with the result that approximately 1.5 percent of all incoming alphas cause a soft error. (This result was for a particularly sensitive 4K test structure.)

The first-order model predicts the error rate to be approximately

$$\begin{aligned}\text{error rate} &= A \times \Phi_\alpha \times S \\ &= (0.027\ \text{cm}^2)\,(3.8\ \alpha/\text{cm}^2 \cdot \text{h}) \\ &\quad (0.015\ \text{errors/alpha}) \\ &= 1.5 \times 10^{-3}\ \text{errors/h} \\ &= 150\ \text{percent/1000 h}.\end{aligned}$$

This predicted value of 150 percent/1000 h is in good agreement with the observed soft error rate of 200 percent/1000 h, obtained in over 200 000 device hours of testing.

Calculations for other devices, including 16K and 64K devices, have also been done. It should be mentioned that second-order effects ignored in this simple model become important for devices which are on the "borderline" of having enough critical charge so as not to fail and for future generations of devices where the cell geometry and the collection efficiency play a more complicated role in determining device sensitivity.

VII. Conclusions and Implications

A new physical mechanism for soft errors in dynamic RAM's and CCD's is the transient upset of dynamic nodes by heavily ionizing radiation from natural package materials surrounding the device. This mechanism is distinct from previously identified sources of random, single-bit errors and is important because of the industry trend toward higher density memory devices with fewer numbers of electrons differentiating between logic states.

This mechanism is expected to impose design and technology restrictions on future generations of devices, particularly at the 64K level and beyond where the charge packet sizes are on the order of several hundred thousand electrons or fewer.

Reduction of alpha flux levels of the glasses, ceramics, and other materials used by the industry will be difficult because of the costs associated with purifying these materials and is unlikely, in any case, to result in the 2-3 orders of magnitude reduction in alpha flux needed for extremely dense memories of the future (if no other corrective actions are taken). Nevertheless, radioactivity reduction programs with major package suppliers are being pursued; inspection of alpha activity of materials will become a difficult matter in itself because of the low fluxes involved.

The most promising area for reducing the soft error rate of future generations of dynamic RAM's and CCD's is that of design and technology changes to reduce device sensitivity.

It is unlikely that all soft errors can be eliminated, especially as the level of integration extends beyond 64K. Thus the use of error detection and correction (EDAC) is increasingly desirable. With single-bit error correction the only problem will be the chance of a soft error occurring in a memory word already containing a hard error; hence the hard error rate will continue to dominate the system MTTF in error-corrected systems.

The density advantage of dynamic MOS memories over static MOS and bipolar memories suggests they will be around for a long time, at ever-increasing levels of integration. The existence of physical obstacles to be overcome as device geometries are reduced represents an interesting challenge for the future.

Acknowledgment

The authors would like to thank the following people for their valuable contributions to the development of the model, to the analysis of materials, and to the testing of devices: C. Barrett, G. Chiu, P. Dahm, P. Engel, M. Geilhufe, N. Khurana, I. Lee, G. Maul, E. Meieran, E. Metzler, J. Miller, W. Oldham, G. Parker, J. SinghDeo, R. Smith, and W. Tchon.

References

[1] U. Fano, "Penetration of protons, alphas particals and mesons," in *Studies in Penetration of Charged Particles in Matter*, National Academy of Sciences–National Research Council, Publication 1133 (Nuclear Science Series–Rep. 39), 1964. Also available in *Handbook of Physics*, E. U. Condon and H. Odishaw, 2nd. ed. New York: McGraw-Hill, 1967.

[2] R. B. Leighton, *Principles of Modern Physics*. New York: McGraw-Hill, 1959, ch. 14.

[3] D. Binder, E. C. Smith, and A. B. Holman, "Satellite anomalies from galactic cosmic rays," *IEEE Trans. Nucl. Sci. (Annual Conf. on Nuclear and Space Radiation Effects)*, vol. NS-22, no. 7, pp. 2675–2680, Dec. 1975.

[4] J. Torkel Wallmark, "Basic considerations in microelectronics," in *Microelectronics; Theory, Design, and Fabrication.* New York: McGraw-Hill, 1963, pp. 25–26.

[5] R. L. Fleischer, P. B. Price, and R. M. Walker, *Nuclear Tracks in Solids: Principles and Applications.* Berkeley, CA: Univ. of California Press, 1975.

[6] J. A. S. Adams and K. A. Richardson, "Thorium, uranium and zirconium concentrations in bauxite," *Economic Geology*, vol. 55, pp. 1653–1675, 1960.

[7] A. O. Woodford, "Radiometric ages," in *Adventures in Earth History*, P. Cloud, ed. San Francisco, CA: W. H. Freeman and Company, 1970.

[8] C. M. Lederer, J. M. Hollander, and I. Perlman, *Table of Isotopes*, 6th ed. New York: Wiley, 1967.